The influence of facing stiffness on the performance of two geosynthetic reinforced soil retaining walls

Richard J. Bathurst, Nicholas Vlachopoulos, Dave L. Walters, Peter G. Burgess, and Tony M. Allen

Abstract: Current limit equilibrium-based design methods for the internal stability design of geosynthetic reinforced soil walls in North America are based on the American Association of State Highway and Transportation Officials (AASHTO) Simplified Method. A deficiency of this approach is that the influence of the facing type on reinforcement loads is not considered. This paper reports the results of two instrumented full-scale walls constructed in a large test facility at the Royal Military College of Canada. The walls were nominally identical except one wall was constructed with a stiff face and the other with a flexible wrapped face. The peak reinforcement loads in the flexible wall were about three and a half times greater than the stiff-face wall at the end of construction and about two times greater at the end of surcharging. The stiff-face wall analysis using the Simplified Method gave a maximum reinforcement load value that was one and a half times greater than the measured value at the end of construction. Furthermore, the surcharge pressure required to reach the creep-limited strength of the reinforcement was about two times greater than the predicted value. The results demonstrate quantitatively that a stiff facing in a reinforced soil wall is a structural component that can lead to significant reductions in reinforcement loads compared to flexible facing systems.

Key words: geosynthetics, retaining walls, reinforced soil, wrapped face, structural facings.

Résumé : Les méthodes courantes de calcul basées sur l'équilibre limite pour les conceptions de stabilité interne des murs en sol armé avec des géosynthétiques en Amérique du Nord utilisent la méthode simplifiée de l'AASHTO. Un défaut de cette approche est qu'elle ne considère pas l'influence du type de parement sur les charges de l'armature. Cet article fait état des résultats de deux murs à pleine échelle instrumentés et construits dans une grande installation d'essais au Collège Militaire Royal du Canada. Les murs étaient essentiellement identiques sauf qu'un mur a été construit avec un parement rigide et l'autre avec un parement flexible enveloppé. Les charges de pic dans l'armature du mur flexible étaient environ 3,5 fois plus grandes que pour le mur rigide à la fin de la construction et environ 2 fois plus grandes à la fin de la mise en place de la surcharge. L'analyse du mur à parement rigide au moyen de la méthode simplifiée a donné une valeur maximale de charge dans l'armature qui était 1,5 fois plus grande que la valeur mesurée à la fin de la construction. De plus, la pression de surcharge requise pour atteindre la résistance limitée par le fluage dans l'armature était d'environ 2 fois plus grande que la valeur prédite. Les résultats démontrent quantitativement que le parement rigide dans un mur en sol armé est une composante structurale qui peut conduire à des réductions appréciables des charges d'armature en comparaison des systèmes à parement flexible.

Mots clés : géosynthétiques, murs de soutènement, sol armé, parement enveloppé, parements structuraux.

[Traduit par la Rédaction]

Introduction

Current North American approaches for the internal stability design of geosynthetic reinforced soil walls are based on the American Association of State Highway and Transportation Officials (AASHTO) Simplified Method (tie-back wedge method) (NCMA 1997; AASHTO 2002; Canadian Geotechnical Society 2006). Recent analysis of the in-service performance of field instrumented geosynthetic reinforced soil retaining walls has shown that this approach leads to excessively conservative design with respect to the number and (or) strength of the reinforcement layers re-

Received 7 November 2005. Accepted 13 July 2006. Published on the NRC Research Press Web Site at http://cgj.nrc.ca on 18 December 2006.

R.J. Bathurst[1] **and N. Vlachopoulos.** GeoEngineering Centre at Queen's-RMC, Department of Civil Engineering, Royal Military College of Canada, Kingston, ON K7K 7B4, Canada.
D.L. Walters. Alston Associates Inc., 85 Citizen Court, Unit 1, Markham, ON L6G 1A8, Canada.
P.G. Burgess. Army Support Unit, Canadian Forces Base Denwood, AB T0B 1B0, Canada.
T.M. Allen. Washington State Department of Transportation, State Materials Laboratory, Olympia, WA 98504–7365, USA.

[1]Corresponding author (e-mail: bathurst-r@rmc.ca).

quired to prevent overstress of the reinforcement (Allen et al. 2002; Allen and Bathurst 2002).

One source of conservatism is the role of stiff structural facings on the magnitude of reinforcement loads. Tatsuoka (1993) characterized wall facings based on their stiffness as follows: Types A and B – very flexible geosynthetic wrapped face, gabion face, or steel skin facings; Type C – articulated (incremental) concrete panels; Type D – full-height precast concrete panels; and Type E – concrete gravity structures. Facing rigidity was defined in terms of local, axial, shear, and bending rigidity, and overall mass as a gravity structure. Tatsuoka (1993) concluded that soil reinforcement strains decrease as facing rigidity increases because of the increase in soil confinement caused by the facing, thereby reducing reinforcement loads.

Allen and Bathurst (2002) analyzed a database of 16 monitored full-scale wall configurations having a range of facing type and geosynthetic reinforcement products. They showed that on average the predicted maximum reinforcement loads using a tie-back wedge method of analysis were about three times greater than values deduced from measured strain readings. A major conclusion of their study was that the discrepancy was due in part to the horizontal load capacity of the concrete facings that were used in most of the walls and not considered in stability analyses. However, the database of monitored walls contained a wide range of contributing factors to wall performance (e.g., range of wall heights, granular soil properties, reinforcement types and layout geometry, amongst other factors). Hence, it was not possible to quantitatively isolate the influence of the facing type on the magnitude of reinforcement loads.

The first phase of a long-term research program at the Royal Military College of Canada (RMC) has been completed that investigates the design and performance of reinforced soil retaining walls during construction, under working load levels, and during uniform surcharge loading approaching wall collapse. The experimental phase of the program involved the construction and testing of 11 full-scale reinforced soil retaining walls in a controlled indoor laboratory environment. Each wall was 3.6 m high and 3.4 m wide with the backfill soil extending approximately 6 m behind the face. Each wall was nominally identical with only one wall parameter varied. The variables were wall facing type, wall facing batter, reinforcement type, and number of reinforcement layers. The results from the test matrix allow the contribution of each component of the wall structure to the overall performance of the composite system to be isolated. Details of the performance of some of the walls in the test series have been reported by Bathurst et al. (2000, 2001, 2002*b*, 2002*c*) and Hatami and Bathurst (2005, 2006).

This paper summarizes the experimental methodology and presents results from two walls that are focused on the influence of facing stiffness on the performance of geosynthetic reinforced soil retaining walls. The two walls were nominally identical structures with the exception that one wall was constructed with a dry-stacked column of concrete modular blocks (very stiff face) and the second with a very flexible wrapped-face construction. The results demonstrate that wall deformations and reinforcement loads are significantly attenuated when a relatively stiff facing is present compared to the idealized case of a very flexible facing. This paper also compares measured maximum reinforcement loads to computed values using a conventional limit-equilibrium tie-back wedge method of analysis. The calculations show that predicted peak reinforcement loads for the flexible wall case using the peak plane strain friction angle of the soil are in reasonable agreement with measured values. However, the same analysis approach for the stiff-face wall gave a maximum reinforcement load value that was a factor of one and a half times greater than the measured value at the end of construction. Furthermore, the surcharge pressure required to reach the creep-limited strength of the reinforcement was about two times greater than the predicted value.

Experimental program

Wall configurations

The walls were constructed in the RMC Retaining Wall Test Facility (Kingston, Ontario). The facility allows full-scale test walls to be constructed and tested under conditions approaching an idealized plane strain condition.

Figure 1 shows a cross-section of the very stiff-face segmental (modular block) wall that was constructed with six layers of the polypropylene (PP) geogrid at a spacing of 0.6 m. The wall was designed to satisfy current National Concrete Masonry Association guidelines (NCMA 1997). An additional design constraint was that the reinforcement layer spacing should not exceed a distance equal to twice the modular block toe to heel dimension (AASHTO 2002). The wall was constructed from the bottom up with no external support for the facing column. The toe of the wall was restrained horizontally but free to rotate. Each course of modular block facing units was placed first, followed by a 150 mm high lift of compacted soil. The wall facing was built with three discontinuous vertical sections with separate reinforcement layers in plan view (i.e., each reinforcement layer was discontinuous in the cross-plane strain direction). The width of the middle wall section was 1 m and it was located between two 1.15 m wide outer sections. The friction between the backfill soil and sides of the test facility was minimized by placing a composite arrangement of plywood, Plexiglas, and lubricated polyethylene sheets over the side walls (Bathurst et al. 2001). The discontinuous wall facing and reinforcement layers, and side wall treatment were used to minimize the frictional effects of the lateral boundaries of the test facility and to allow the instrumented middle section of the wall structure to approach a plane strain test condition as far as practical.

Figure 2 illustrates the cross-section of the nominally identical wall but with the reinforcement arranged to form a very flexible wrapped face. The wall was constructed on a thin (100 mm thick) sand leveling layer to lift the first reinforcement layer above the concrete foundation. Hence, each reinforcement layer in this wall was 200 mm below the corresponding layer in the segmental stiff-face wall. This small difference in elevation was not expected to complicate quantitative comparisons of the performance of the two walls. The shaded zone close to the face of the structure in Fig. 2 corresponds to the cross-section occupied by the equivalent stacked modular block facing in the segmental wall. Each facing wrap was attached to the reinforcement layer above using a metal bar clamp. With the exception of the top layer,

Fig. 1. Cross-section of stiff-face (segmental) reinforced soil retaining wall.

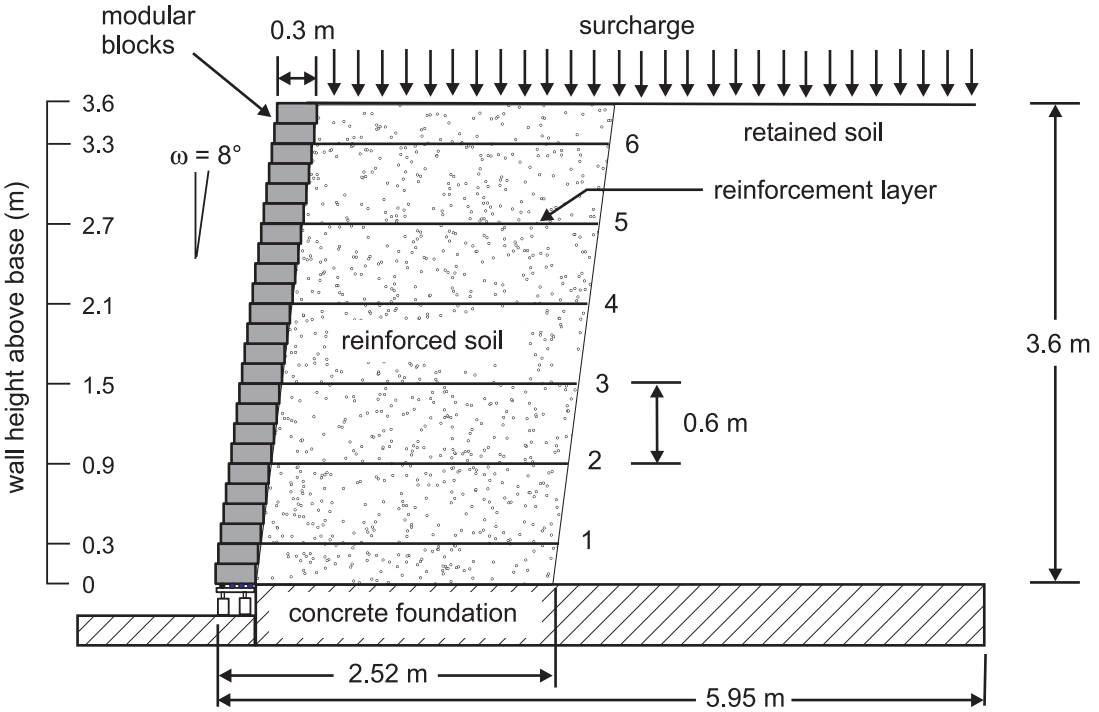

Fig. 2. Cross-section of flexible wrapped-face reinforced soil retaining wall.

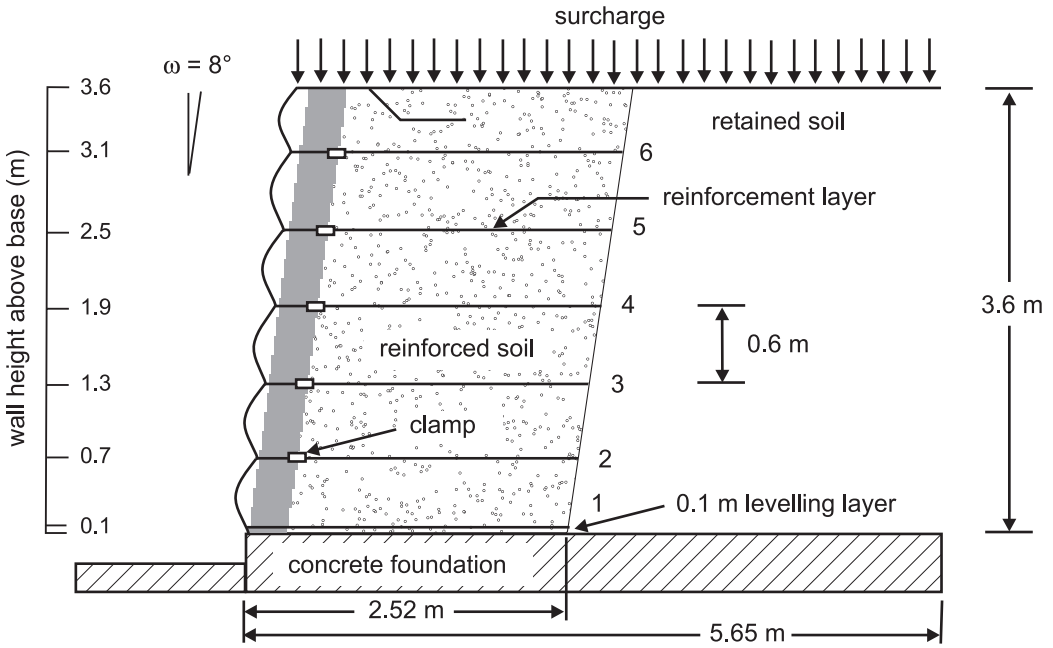

each facing wrap was not extended back into the reinforced soil zone. Hence, the geometry and reinforcement attachment used in this wall does not correspond to a typical wrapped-face construction in the field. The construction technique used in this investigation was purposely adopted to facilitate quantitative comparison of a wall built with a stiff face and a nominally identical wall built with an idealized very flexible face. A "moving formwork" was used in the construction of the wrapped-face wall, which is a common construction technique in the field (Holtz et al. 1997). The forms were braced against the front of the test facility to maintain a target facing batter of $\omega = 8°$ from the vertical. Two wrapped-face layers were supported simultaneously during construction. For example, while layer 4 and the associated wrapped-face section were being constructed, layer 3 and the wrapped face between layers 3 and 4 were supported, and the bottom 1.3 m height of wall was left unbraced. A lightweight woven geotextile was placed inside the geogrid wrapped face to prevent the sand backfill from escaping through the front of the wall. To isolate the central

instrumented section of the wall, each reinforcement layer beyond the bar clamps was trimmed to be discontinuous in plan view as described earlier for the stiff-face wall.

Figure 3 shows the instrumentation used to measure the performance of the stiff-face wall at the end of construction and during staged uniform surcharging. More than 300 instruments were monitored including displacement-type potentiometers, vertical settlement plates, soil strain inductance coils, load rings and load cells, earth pressure cells, and wire-line extensometers and strain gauges attached directly to the reinforcement layers. Further details of the instrumentation program are reported by Bathurst et al. (2000, 2001, 2002*b*, 2002*c*).

Soil

Figure 4 shows the particle size distribution curve for the sand backfill used in the tests. The material was a uniformly graded, naturally deposited rounded beach sand (SP according to the Unified Soil Classification System) with D_{50} = 0.34 mm, coefficient of curvature C_c = 2.25, and coefficient of uniformity C_u = 1.09. The fines content (particle sizes < 0.075 mm) was less than 1%. Hatami and Bathurst (2005) reported the results of direct shear tests for the same sand used in this investigation and under confining pressures representative of vertical stress levels in the two walls. They reported the peak direct shear friction angle as $\phi_{ds} = 41°$ and constant volume friction angle as $\phi_{cv} = 35°$. The (secant) peak plane strain friction angle was also determined directly from plane strain (biaxial) compression tests carried out under similar load levels and reported as $\phi_{ps} = 44°$, (called the peak plane strain friction angle in this paper). This value was shown by Hatami and Bathurst (2005) to be the same value predicted by Bolton's equation (Bolton 1986) using direct shear test results. The three secant friction angle values reported here have been used in computations reported later in the paper. The most conservative value for design is clearly the constant volume value (ϕ_{cv}). In current design practice, the peak value from direct shear tests (ϕ_{ds}) is commonly recommended. However, peak plane strain values are typically higher than values deduced from direct shear tests (Jewell 1989). Hence, to minimize the level of conservatism in predicted reinforcement loads using a conventional tie-back wedge method because of the choice of friction angle, the plane strain value (ϕ_{ps}) was also used.

The sand has a flat compaction curve and was compacted using a light-weight vibrating mechanical plate compactor in 150 mm lifts to a bulk unit weight of 16.7 kN/m^3 at a moisture content of 3% to 5%. However, the first 0.5 m distance directly behind the wall facing was hand tamped to the same density using a rigid steel plate. This precautionary measure was taken to minimize construction-induced outward deformation and to reduce compaction-induced lateral stresses against the back of the facing.

Reinforcement

The geosynthetic reinforcement product used in the construction of the walls was a relatively weak, biaxially drawn PP geogrid that was oriented in the weak direction. Each layer of geogrid had a total length of 2.52 m measured from the front of the facing column. The aperture size for the PP reinforcement was 25 mm between longitudinal members and 33 mm between transverse members.

In-isolation constant load (creep) tests were carried out on specimens of geogrid in accordance with the ASTM (2004) protocol for maximum durations up to 1000 h or 2000 h. The tests were carried out at a temperature of 20 ± 1 °C, matching the soil temperature in the test walls. The constant load (creep) curves for the reinforcement are plotted in Fig. 5*a*. The data are replotted in Fig. 5*b* as isochronous load–strain curves using the method described by McGown et al. (1984*a*). The initial linear portion of each plot is restricted to very low load levels (less than 1 kN/m). The plots are highly nonlinear, which is consistent with the nonlinear viscoelastic-plastic behaviour expected from drawn PP geogrid products when subjected to tensile loading. Superimposed on Fig. 5*b* is the index load–strain plot for the same material from a constant rate of strain (CRS) wide-width strip tensile test carried out at a strain rate of 10%/min (ASTM 1986). The index strength of the reinforcement at 5% strain was approximately 9 kN/m with an ultimate strength of about 13 kN/m. This reinforcement product is at the very low end of stiffness and strength that is typically specified for geosynthetic reinforced soil walls in the field. This product was purposely selected to generate detectable strains in the reinforcement and to encourage large wall deflections using the available surcharge capacity of the test facility.

The isochronous load–strain data in Fig. 5*a* are used to create the secant stiffness (J) curves plotted at the bottom of Fig. 5*c*, as recommended by Walters et al. (2002). These curves can be used to calculate the tensile load (T) in the reinforcement according to $T = J(t, \varepsilon) \times \varepsilon$, where T is the tensile load in kN/m width of specimen, ε is the strain, and t is time (i.e., duration of loading). The data have been extrapolated to strain values less than 1% and for load durations up to 2000 h and 3000 h. Superimposed on the same plot are secant stiffness values calculated from the reference CRS test. The plot shows that at 2% strain the CRS test overestimates the stiffness of the reinforcement by a factor of 2.6.

Figure 5*d* shows a Sherby Dorn plot constructed from the creep data. The curves in the figure show that there is a significant change in the long-term response of the reinforcement at a load level of about 3.9 kN/m. This load level is referred to hereafter as the "creep-limited strength" of the reinforcement. This value is understood to be a performance limit state since constant tensile loads in excess of this will lead to rupture over time (McGown et al. 1984*b*; WSDOT 2005).

Segmental units

The modular facing units for the segmental wall were a solid masonry block with a continuous concrete shear key. The blocks were 300 mm long (toe to heel), 150 mm high, 200 mm wide, and had a mass of 20 kg. The wall facing units were built with a staggered (running joint) pattern matching the construction technique used in the field. During wall construction the shear keys aid in maintaining the target wall batter at (or close to) $\omega = 8°$ from vertical.

Construction and surcharge loading

The construction and surcharging history of each wall is illustrated in Fig. 6. Following construction, each wall was

Fig. 3. Instrumentation arrangement for stiff-face retaining wall.

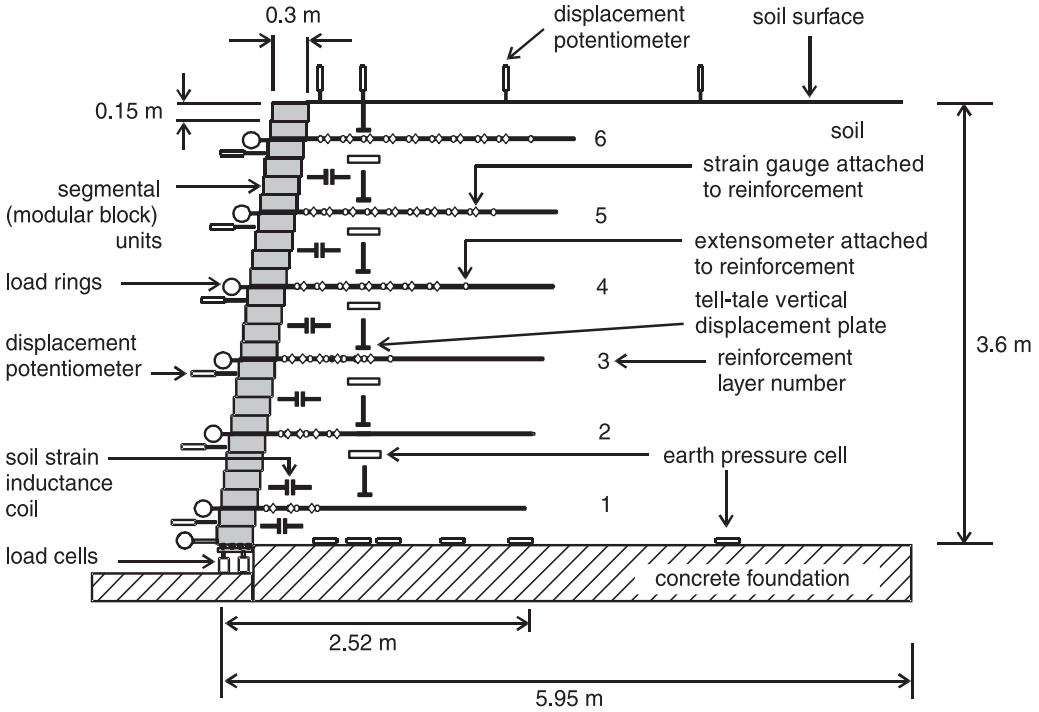

Fig. 4. Particle-size distribution for backfill sand.

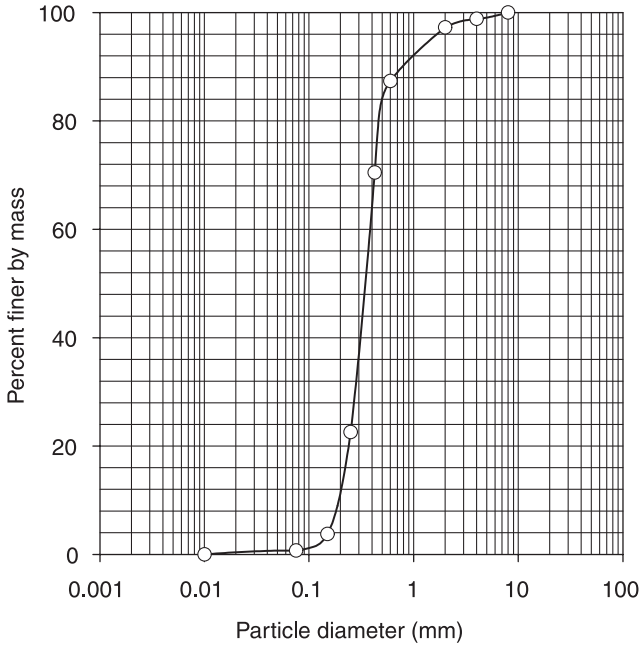

stage uniform surcharged using a system of airbags placed over the entire surface of the backfill soil. Each constant surcharge load increment was applied for 25 h to 400 h to monitor time-dependent deformations in the wall. The vertical axis on the left-hand side of the plot represents the equivalent height of the wall calculated as q/γ, where q is the applied surcharge pressure and γ is the bulk unit weight of the backfill soil. The right-hand side vertical axis is the computed base pressure at the foundation. The surcharging was continued until excessive outward deformations of the wall face and large strains in the reinforcement layers were recorded and (or) the surcharge capacity of the test facility was reached. It can be noted in Fig. 6 that the walls were constructed and loaded at different rates. However, at the end of each test the duration of wall construction and surcharging was similar at about 3500 h.

Measured performance

Facing displacements

Figure 7 shows the facing column profile for both walls at the end of construction based on manual surveys. The dashed straight line at the right in the figure is the target facing batter based on the geometry of the block units and the built-in concrete shear key location. This is the profile of the stiff-face wall if the blocks could be placed without backfill and each unit pushed forward against the shear keys on the underlying blocks. The figure shows that the actual facing alignment for the segmental wall is steeper than the target batter as a result of the incremental construction of the facing column together with fill placement and compaction. The maximum out-of-alignment deformation from the target batter was about 3% of the wall height.

The very flexible wrapped-face wall can be seen to have displaced by about 250 mm at the base of the wall at the end of construction. This movement was generated largely at the time the bottom formwork was removed after construction of the two lowermost layers of reinforcement. However, the final facing slope was reasonably constant at the target batter value of 8°.

The influence of facing rigidity on wall deformations is illustrated in Fig. 8 using measurements of the maximum outward deformation of each wall taken during post-construction surcharging. The maximum facing dis-

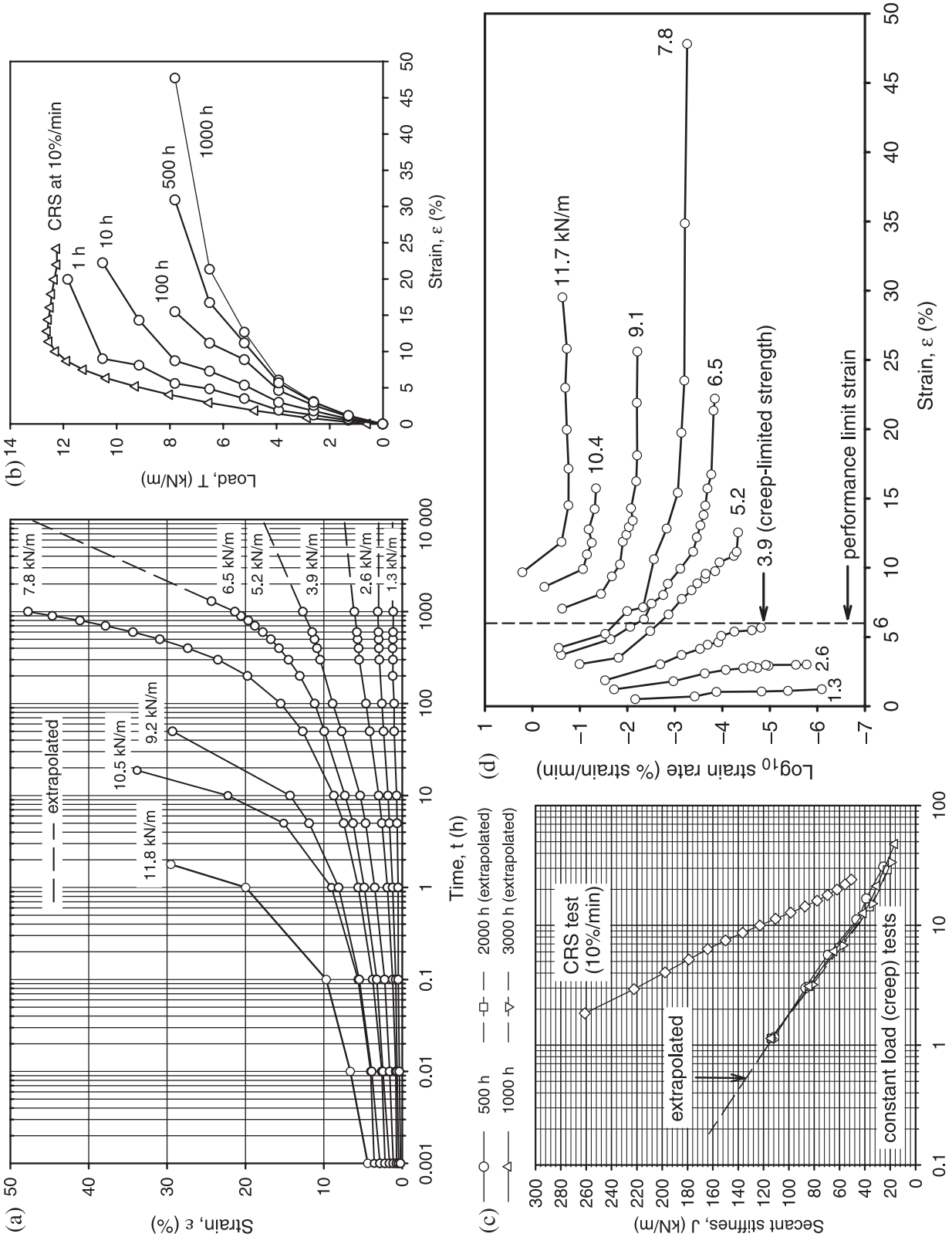

Fig. 5. Results of in-air testing of PP geogrid specimens. (*a*) Constant load (creep) tests. (*b*) Isochronous load–strain curves and results of constant rate-of-strain (CRS) test. (*c*) Secant stiffness of geogrid reinforcement. (*d*) Sherby Dorn plot.

Fig. 6. Construction and surcharging history for test walls with respect to the beginning of construction.

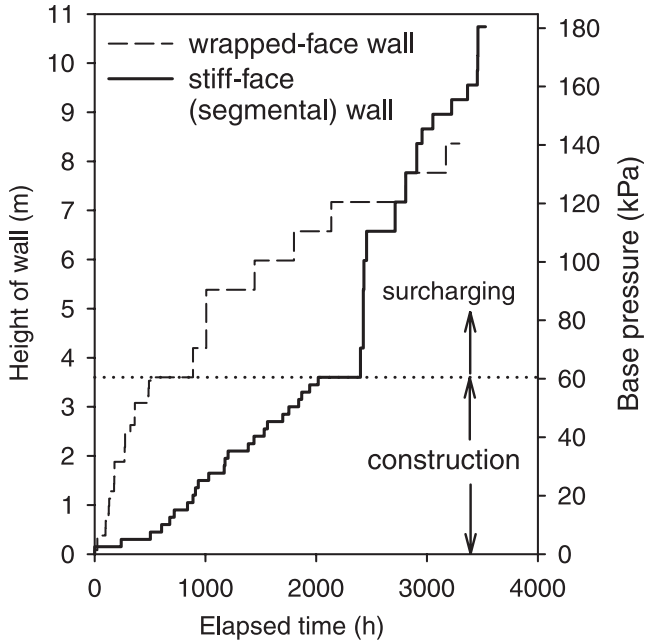

Fig. 7. Facing profiles at end of construction.

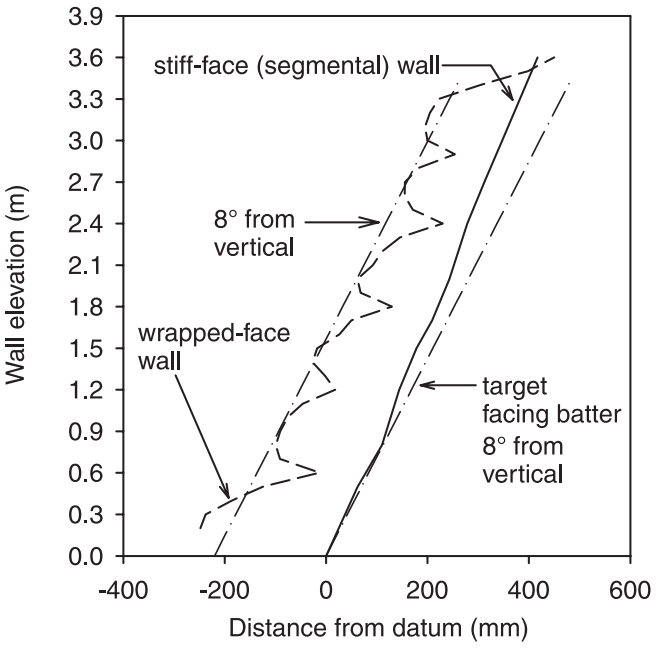

placements have been calculated with respect to the end-of-construction profile for each wall and both occurred at about 3 m above the toe of the wall. The discrete modular facing construction for the stiff-face wall resulted in some unevenness in outward deformations at each monitored elevation. Hence, the readings recorded in the figure for this structure are the maximum, minimum, and average values recorded at the same elevation on the face over the central instrumented section of wall.

At a common surcharge pressure of 80 kPa, the maximum post-construction facing displacement for the wrapped-face

Fig. 8. Maximum post-construction outward deformation of wall facing recorded at a height of 3 m above the wall toe.

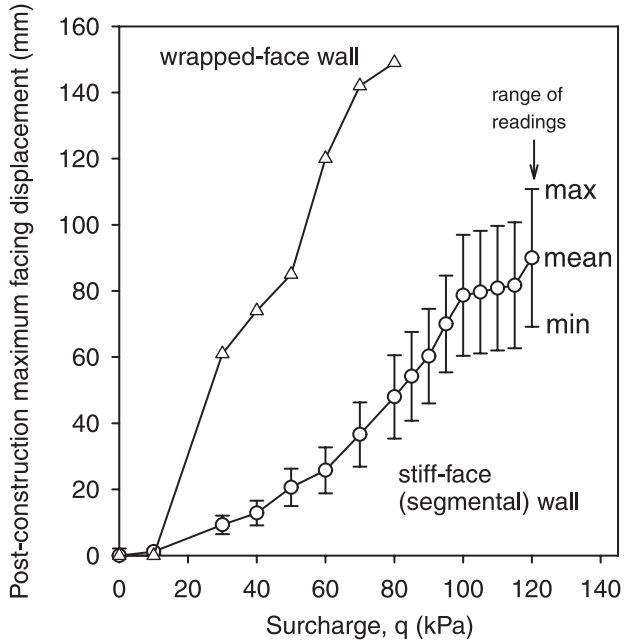

wall was three times greater than that recorded for the stiff-face wall. Hence, the data in Figs. 7 and 8 clearly show that the stiff face restrained the lateral movement of the soil during the construction and surcharge loading of this wall. Figure 8 also shows nonlinear and irregular displacement responses for the walls during surcharging. This is consistent with the strain level dependent isochronous stiffness of the reinforcement (Fig. 5*b*) and the onset of soil failure at large surcharge loads.

Reinforcement strains

Figure 9*a* compares the strain magnitude and distribution in the six layers of reinforcement at the end of construction for both walls determined from strain gauge readings and strains inferred from pairs of extensometer points mounted on the reinforcement layers. Strain gauge readings were used for strains less than 2%. At higher strain levels the strain gauges debonded from the reinforcement surface, and strains were calculated using adjacent pairs of extensometer points. The range bars in the figure represent ± 1 standard deviation based on estimates of measured strains from multiple readings taken at nominally identical distances behind the facing of each wall (Bathurst et al. 2002*a*). The coefficient of variation for strain measurements (COV_ε) calculated from strain gauges and extensometer pairs ranged from 53% to 9%. The larger value was applied to low values of strain from strain gauge readings and the lower value to larger strains taken from extensometer readings.

The data show that the strain magnitudes are very small for the stiff-face structure (less than 1%) but much larger for the wrapped-face structure (maximum of 4%). The largest measured strains occurred close to the facing for both walls. The strains for the wrapped-face wall were as great as four times the magnitude of the strains recorded for the modular

Fig. 9. Reinforcement strains. (*a*) End of construction. (*b*) 80 kPa surcharge. Range bars represent ± 1 standard deviation on measured strains.

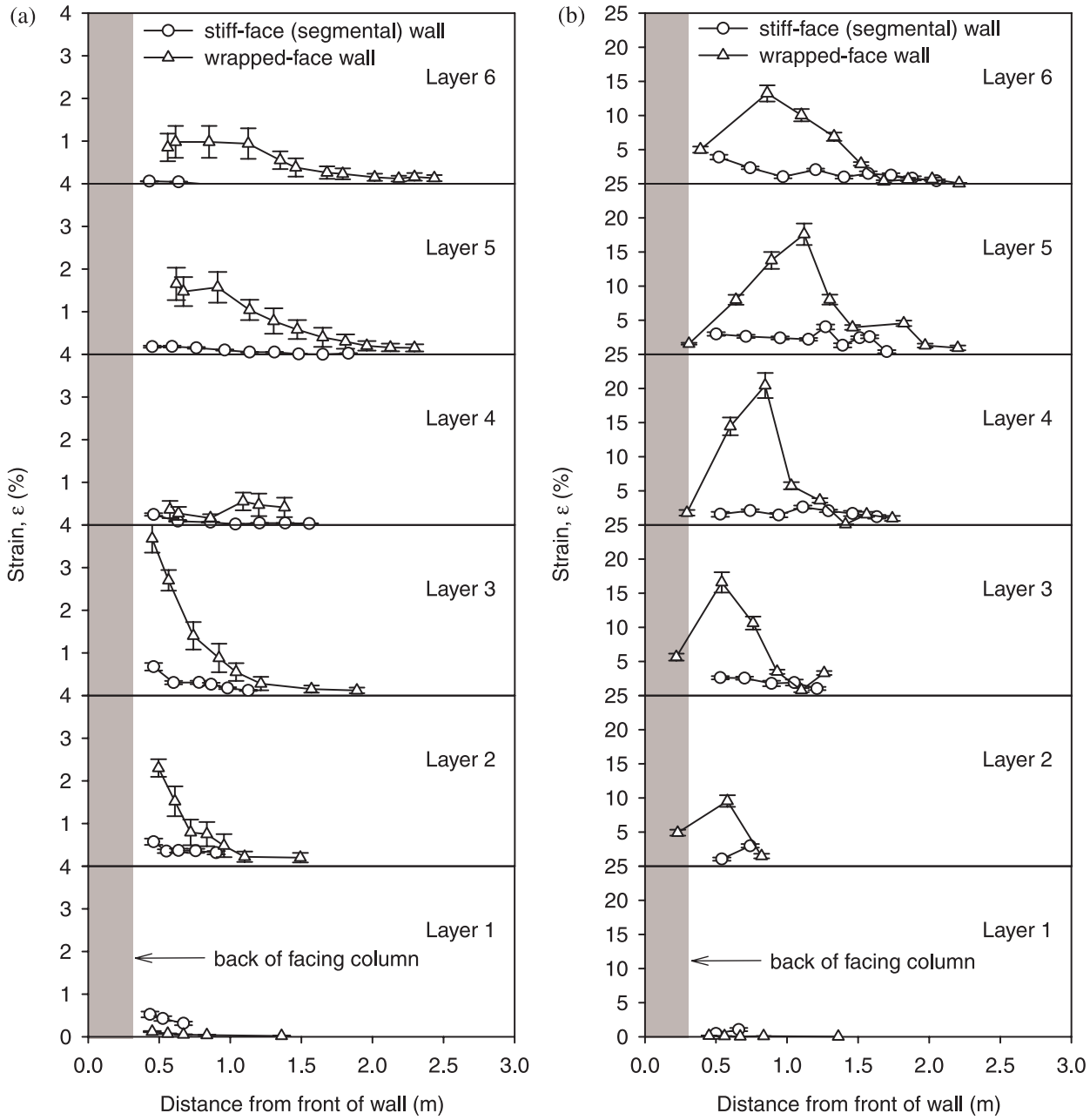

block structure, suggesting that the rigid facing carries a significant portion of the lateral earth loads.

The relatively high strains at the connections with the stiff-face wall can be attributed to the downward movement of the soil behind the facing. This movement occurs as a result of settlement of the backfill during compaction and outward rotational movement of the facing column during construction (Fig. 7). The high strains recorded at the same location in the wrapped-face wall are due to the downward sagging of the wrapped portions at the front of the wall (Fig. 7). A similar pattern of peak strains close to the face has been reported by Bathurst et al. (1988) for a wrapped-face wall at the end of construction. This earlier wall was constructed using a similar reinforcement material but with a reinforcement spacing of 750 mm and no artificial clamping of the reinforcement layers as described earlier.

Figure 9*b* shows that strain magnitudes are up to five times larger for each wall at the 80 kPa surcharge load compared to the end-of-construction strains in Fig. 9*a*. The comparison at the 80 kPa surcharge load level was chosen because it was the highest load applied to the wrapped-face structure. The results show that there was no clearly defined peak location of strain along each reinforcement layer in the stiff-face wall at this surcharge load level. Only after the surcharge reached 90 kPa did a local peak reinforcement strain develop at a location on the reinforcement corresponding to a contiguous internal failure plane in the reinforced soil zone. However, clearly defined peak strain locations and

larger strains in each reinforcement layer were observed for the wrapped-face wall at this surcharge load level. This is consistent with the notion of an internal failure surface (or surfaces) propagating through the reinforced soil zone. Based on the analysis of data obtained from backfill soil surveys taken during wall excavation, it was determined that the shape of the internal soil shear failure surface could be approximated by a log spiral curve propagating from the toe of the wall.

Reinforcement tensile loads

Figures 10*a* and 10*b* show the measured reinforcement loads in the highest loaded reinforcement layer in the stiff-face (segmental) wall and the flexible wrapped-face wall, respectively. The calculation of "measured" reinforcement load, T, was based on the isochronous stiffness value, J, and measured strain value, ε, for the target layer at the time of interest using the data in Fig. 5*c* and the method described in the section entitled "Reinforcement". The duration of loading, t, was taken as the elapsed time since the layer was placed in the wall. The same isochronous stiffness values have been used to successfully predict the measured reinforcement loads at the connections in the RMC test walls (Walters et al. 2002). A nonlinear load–strain – time-reinforcement model based on the same approach was also implemented in a numerical code by Hatami and Bathurst (2006) to predict the quantitative response of several RMC test walls at the end of construction and during surcharging. Computed results were within measurement accuracy.

Associated with each load value is uncertainty in the predicted load value, which varies with the magnitude of the estimate of error of the measured strain in the reinforcement and the stiffness value from in-isolation creep data. The upper limit on the coefficient of variation of the reinforcement stiffness value (COV_J) for the PP geogrid in this investigation was calculated to vary between 5% and 13% based on data presented by Walters et al. (2002). Uncertainties in strain measurements (COV_ε) and stiffness values (COV_J) are uncorrelated (i.e., independent). Therefore, total uncertainty in estimated reinforcement loads can be quantified by a coefficient of variation (COV_T) value calculated as follows (Ang and Tang 1975):

$$[1] \qquad COV_T = \sqrt{COV_\varepsilon^2 + COV_J^2}$$

This approach is used to calculate the range bars in Figs. 10*a* and 10*b* for measured reinforcement load values. Additional variation due to potential installation damage and (or) environmental degradation, as would be the case for the design of a field structure, was not required in this study. Bush and Swan (1988) demonstrated that for polyolefin geogrid reinforcement materials used in the walls constructed in the RMC facility, there was no deterioration in stiffness values. This is not unexpected given the careful construction technique, the light-weight compaction equipment employed in these test walls, and the benign soil environment.

Also shown in Figs. 10*a* and 10*b* are predicted maximum reinforcement load values, T_{max}, using the "tie-back wedge method" (AASHTO 2002; NCMA 1997) calculated as

$$[2] \qquad T_{max} = S_v K_{ah}(z\gamma + q)$$

where S_v is the tributary area (equivalent to the vertical spacing of the reinforcement when analyses are carried out per unit length of wall); $K_{ah} = f(\phi, \delta, \omega)$ is the horizontal component of active lateral earth pressure coefficient calculated according to Coulomb earth pressure theory; ϕ is the peak friction angle of the soil; δ is the peak wall–soil interface friction angle; ω is the wall facing batter from the vertical; γ is the soil bulk unit weight; z is the depth of the reinforcement layer below the crest of the wall; and q is the uniform surcharge pressure applied to the backfill surface. This approach can be understood to be a limit-equilibrium method that assigns a portion of the Coulomb earth pressure distribution to each layer based on the reinforcement spacing.

In AASHTO (2002) and Canadian Geotechnical Society (2006) guidelines, the contribution of soil–wall interface friction and facing batter is ignored. As an initial effort to improve agreement between predicted reinforcement loads using the tie-back wedge method and measured values from instrumented field walls, Allen and Bathurst (2002) recommended including interface friction and wall batter in the calculation of the horizontal component of active earth pressure (Modified AASHTO Simplified Method). This is the same approach adopted by the National Concrete Masonry Association (Bathurst and Simac 1994; NCMA 1997) for the design of reinforced soil modular block retaining walls. The Modified AASHTO Simplified Method is used in the calculation of reinforcement loads to follow.

Predicted load values have been calculated using three different peak friction values for the backfill soil ($\phi = \phi_{ps} > \phi_{tds} > \phi_{tv}$) determined from laboratory direct shear and plane strain tests (see section entitled "Soil") and $\delta = \phi$. Note that in this calculation the facing column is assumed to create a soil-to-soil interface inclined at $\omega = 8°$ for the wrapped-face wall and located 0.3 m from the face of the wall (i.e., at the location of the clamps shown in Fig. 2). Predicted load values at each surcharge load level can be seen to decrease with increasing peak friction angle, as expected using Coulomb earth pressure theory. The peak friction angle (ϕ_{tds}) from direct shear tests (or conventional triaxial compression tests) is specified in current North American practice (NCMA 1997; AASHTO 2002). Allen et al. (2002) have proposed that the peak plane strain angle (ϕ_{ps}) be used in current reinforced soil wall design practice (tie-back wedge method) since wall geometry typically conforms to a plane strain condition. Furthermore, lower reinforcement loads are predicted, which reduces the discrepancy with observed loads in field walls that have been inferred from measured strains.

The data for the stiff-face (segmental) wall in Fig. 10*a* shows that the least discrepancy between predicted and measured reinforcement loads at all surcharge levels corresponds to calculations using the peak plane strain friction angle ($\phi = \phi_{ps}$). The magnitude of the discrepancy between predicted and measured results increases as the value of ϕ decreases.

Superimposed on the figure is the creep-limited strength (3.9 kN/m from Fig. 5*d*). It should be noted that no reduction in the available strength of the reinforcement to account for installation and (or) environmental degradation was required for the reasons noted earlier.

Fig. 10. Predicted and measured maximum reinforcement tensile loads at the end of construction and during surcharging for (*a*) stiff-face segmental wall and (*b*) flexible wrapped-face wall.

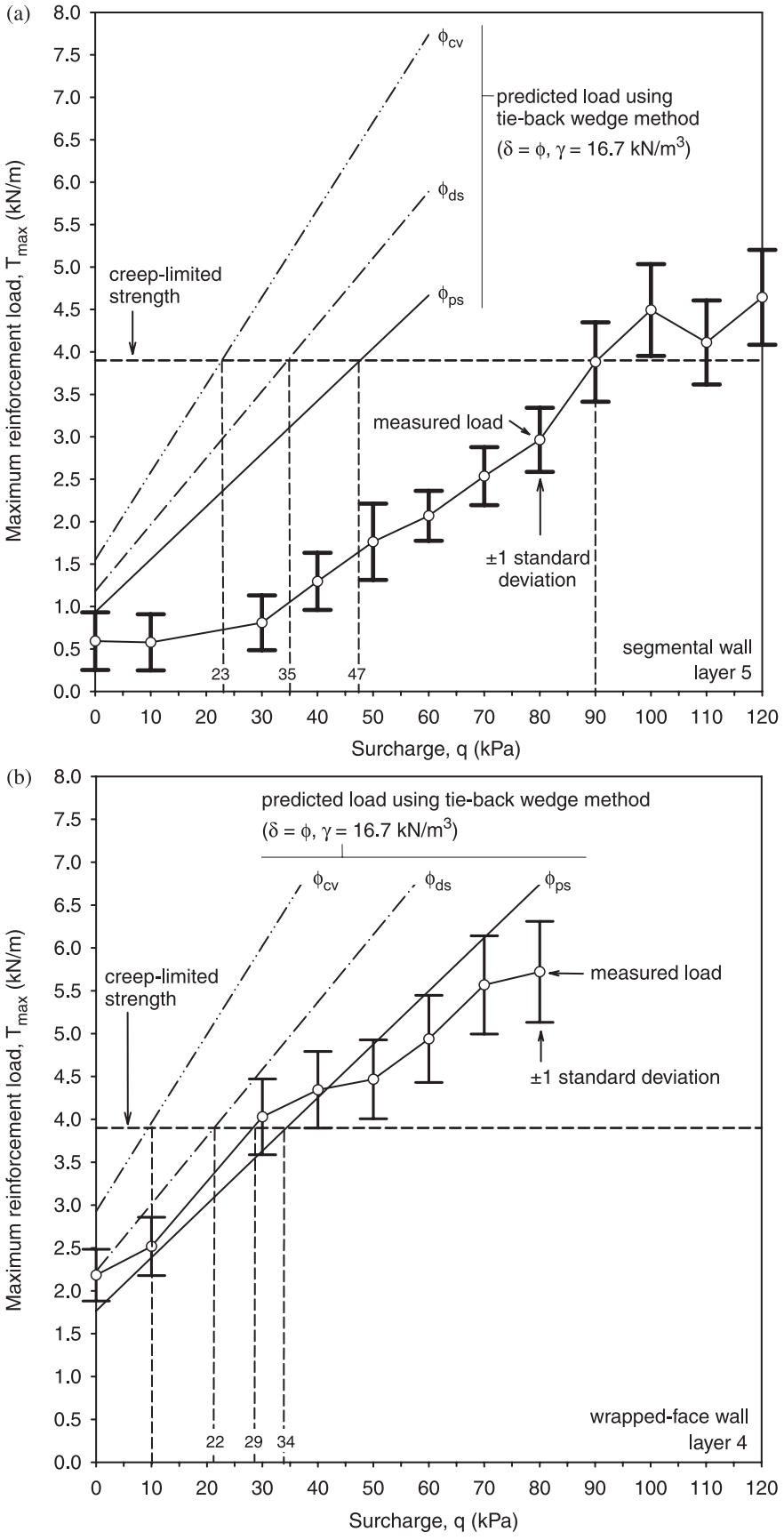

The creep-limited strength value is a limit state for design since it represents a load level in the reinforcement that if sustained over a long period of time can be expected to lead to strain to rupture of the layer. The measured data shows that the creep-limited strength of the critical reinforcement layer in this wall was reached at a surcharge load of 90 kPa, while predicted surcharge levels to reach this limit state are 47 kPa, 35 kPa, and 23 kPa for calculations carried out with ϕ equal to ϕ_{ps}, ϕ_{ds}, and ϕ_{cv}, respectively. Hence, the surcharge load level required to reach this limit state is underpredicted by a factor of 1.9, 2.6, and 3.9 for the stiff-face wall structure using ϕ equal to ϕ_{ps}, ϕ_{ds}, and ϕ_{cv}, respectively.

A similar set of data is shown in Fig. 10*b* for the flexible wrapped-face wall structure. The surcharge load level to reach the creep-limited strength limit state is 29 kPa, which is a factor of 3.1 lower than the value of 90 kPa for the nominally identical stiff-face wall. This difference is ascribed to the relatively low facing column stiffness for the flexible wrapped-face wall structure. It can be noted that the tie-back wedge method using the peak plane strain friction angle ($\phi = \phi_{ps}$) gives reasonably accurate estimates of measured reinforcement loads (i.e., generally within ± 1 standard deviation of the mean measured load value) for surcharge levels up to 50 kPa. At end of construction the peak direct shear value calculation with $\phi = \phi_{ds}$ gives a value of maximum reinforcement load that matches the measured value but overestimates the measured values during subsequent surcharging. Within experimental error it can be argued that the surcharge load to reach the creep-limited strength value of the reinforcement falls within limits predicted using peak direct shear and peak plane strain friction angles for the soil ($\phi_{ds} = 41°$ and $\phi_{ps} = 44°$, respectively). Calculations using $\phi = \phi_{cv}$ underestimated the surcharge load level to achieve the creep-limited strength of the critical layer by a factor of 2.9.

However, it should be noted that the wrapped-face wall is an unusually flexible structure. Wrapped-face wall structures in practice are constructed with facing wraps that extend into the reinforced soil zone, and this can be expected to give a stiffer facing performance. The soil reinforcement material used in this test wall was also very extensible. Hence, the surcharge pressure to achieve the same performance limit state can be expected to be greater for a similar height wrapped-face structure in the field constructed with stiffer geogrid reinforcement. Consequently, it may be expected that the agreement between predicted peak maximum reinforcement load and the measured load would be best using a peak plane strain friction angle for a wall built with facing wraps that extend back into the soil.

Conclusions and discussion

The following conclusions can be made from the work described in this paper:

(1) In this investigation, the reinforcement strains in the flexible wrapped-face wall were as great as five times those recorded for the stiff-face wall. When peak reinforcement strains are converted to loads using a suitability selected isochronous stiffness value, the peak loads in the reinforcement for the flexible wall were about 3.5 times greater than the stiff-face wall at the end of construction and about two times greater at the end of surcharging (q = 80 kPa).

(2) The maximum predicted reinforcement load for the stiff-face wall using a tie-back wedge method (NCMA 1997) and the peak plane strain friction angle of the soil was a factor of one and a half times greater than the measured value at the end of construction. The surcharge pressure required to reach the creep-limited strength of the reinforcement was about two times greater than the predicted value.

(3) For the very flexible wrapped-face wall in this research program, the tie-back wedge method slightly overpredicted the reinforcement loads up to the creep-limited strength of the critical reinforcement layer during surcharging using the soil peak direct shear friction angle, and it slightly underpredicted the reinforcement loads using the soil peak plane strain friction angle. However, over the entire surcharge load range, the measured peak reinforcement loads were in reasonable agreement with computed values using the peak plane strain friction angle.

The quantitative observations made above support the hypothesis that a rigid facing column of the type used in this investigation is a structural element that acts to reduce the magnitude of wall deformations and reinforcement strains that would otherwise develop in a wall with a perfectly flexible facing. The contribution of the rigid facing to reinforcement strain (or load) is not accounted for in the current Simplified Method for reinforced soil retaining walls including segmental retaining walls (NCMA 1997; AASHTO 2002; Canadian Geotechnical Society 2006).

The use of peak soil shear strength versus residual shear strength for granular backfills in geosynthetic reinforced soil wall design has been the subject of debate (e.g., Leshchinsky 2003) and is beyond the scope of this paper. However, in the current investigation, the use of a constant volume (residual) friction angle clearly gave the most conservative predictions of the maximum reinforcement load in both walls at the end of construction and during subsequent surcharging.

The reduction of reinforcement loads due to the presence of a rigid facing column cannot be easily implemented in the tie-back wedge method, which is based on force equilibrium. A strategy to explicitly include the effect of facing rigidity on maximum reinforcement loads under working load levels has been proposed by Allen et al. (2003) and Bathurst et al. (2005) using an empirical approach (*K*-stiffness method). In their design method the maximum reinforcement load in a flexible wrapped-face wall may be up to three times as great as an otherwise nominal identical wall constructed with a very stiff concrete facing column. This factor of three was determined from back-analysis of 20 full-scale instrumented field walls with 35 different wall sections. The relative load levels deduced for the two walls in this experimental program at the end of construction are consistent with field data reported in the previous studies noted here.

A practical implication of the current investigation and previous related studies is that current design practice leads to selection of excessively strong (or) stiff geosynthetic reinforcement products when used in combination with a stiff structural facing. For wrapped-face wall construction, however, the discrepancy is much less and indeed the Modified

AASHTO Simplified Method is likely sufficiently accurate if the soil peak plane strain friction angle is used in computations.

Acknowledgements

The financial support for this study was provided by the Natural Sciences and Engineering Research Council (NSERC) of Canada and the following US State Departments of Transportation: Alaska, Arizona, California, Colorado, Idaho, Minnesota, New York, North Dakota, Oregon, Utah, Washington, and Wyoming. The writers also acknowledge the financial support from the Academic Research Program of the Department of National Defence (Canada) and operating grants from the Department of National Defence, Canada. The writers are also grateful for the financial support of the National Concrete Masonry Association and the contribution of materials by Risi Stone Systems (Thornhill, Ontario) and Terrafix Inc. (Toronto, Ontario).

References

AASHTO. 2002. Standard specifications for highway bridges. American Association of State Highway and Transportation Officials, 17th ed., Washington, D.C.

Allen, T.M., and Bathurst, R.J. 2002. Soil reinforcement loads in geosynthetic walls at working stress conditions. Geosynthetics International, **9**(5–6): 525–566.

Allen, T.M., Bathurst, R.J., and Berg, R.R. 2002. Global level of safety and performance of geosynthetic walls: An historical perspective. Geosynthetics International, **9**(5–6): 395–450.

Allen, T.M., Bathurst, R.J., Holtz, R.D., Walters, D., and Lee, W.F. 2003. A new working stress method for prediction of reinforcement loads in geosynthetic walls. Canadian Geotechnical Journal, **40**(5): 976–994.

Ang, A.H.-S., and Tang, W.H. 1975. Probability concepts in engineering planning and design: Vol. 1 – Basic principles. John Wiley & Sons, New York, N.Y.

ASTM. 1986. Standard test method for tensile properties of geotextiles by the wide-width strip method (D4595–86). CD ROM annual book of ASTM standards. Vol. 4.13. American Society for Testing and Materials, West Conshohocken, Penn.

ASTM. 2004. Standard test method for evaluating the unconfined tension creep and creep rupture behaviour of geosynthetics (D5262–04). CD ROM annual book of ASTM standards. Vol. 4.13. American Society for Testing and Materials, West Conshohocken, Penn.

Bathurst, R.J., and Simac, M.R. 1994. Geosynthetic reinforced segmental retaining wall structures in North America. Keynote paper. *In* Proceedings of the 5th International Conference on Geotextiles, Geomembranes and Related Products, 6–9 September 1994, Singapore. Southeast Asia Chapter of the International Geosynthetics Society, Singapore. Vol. 4, pp. 1275–1298.

Bathurst, R.J., Jarrett, P.M., and Lescoutre, S.R. 1988. An instrumented wrap-around geogrid wall. *In* Proceedings of the 3rd Canadian Symposium on Geosynthetics, Kitchener, Ont. Canadian Geotechnical Society, Alliston, Ont. pp. 71–78.

Bathurst, R.J., Walters, D., Vlachopoulos, N., Burgess, P., and Allen, T.M. 2000. Full scale testing of geosynthetic reinforced walls. Keynote paper. *In* Proceedings of Geo-Denver 2000. *Edited by* J.G. Zornberg and B.R. Christopher. American Society of Civil Engineers, Geotechnical Special Publication No. 103, pp. 201–217.

Bathurst, R.J., Walters, D.L., Hatami, K., and Allen. T.M. 2001. Full-scale performance testing and numerical modelling of reinforced soil retaining walls. Special plenary lecture. *In* Proceedings of International Symposium on Earth Reinforcement, IS Kyushu 2001, Fukuoka, Japan, 14 November 2001. *Edited by* H. Ochiai, J. Otani, N. Yasufuku, and K. Omine. A.A. Balkema, Rotterdam, The Netherlands. Vol. 2, pp. 777–799.

Bathurst, R.J., Allen, T.M., and Walters, D.L. 2002*a*. Short-term strain and deformation behaviour of geosynthetic walls at working stress conditions. Geosynthetics International, **9**(5–6): 451–482.

Bathurst, R.J., Walters, D.L., Esfehani, M., El-Emam, M., and Blatz, J.A. 2002*b*. Physical modelling of geosynthetic walls and embankments. Keynote paper. *In* Proceedings of International Conference on Physical Modeling in Geotechnics (ICPMG), St. Johns, Newfoundland, 10–12 July 2002, A.A. Balkema, Lisse, The Netherlands. pp. 21–30.

Bathurst R.J., Walters, D.L., Hatami, K., Saunders, D.D., Vlachopoulos, P., Burgess, P.G., and Allen, T.M. 2002*c*. Performance testing and numerical modelling of reinforced soil retaining walls. *In* Proceedings of the 7th International Conference on Geosynthetics, Nice, France, 22–27 September 2002, A.A. Balkema, Lisse, The Netherlands. Vol. 1, pp. 217–220.

Bathurst, R.J, Allen, T.M., and Walters, D.L. 2005. Reinforcement loads in geosynthetic walls and the case for a new working stress design method. Geotextiles and Geomembranes, **23**: 287–322.

Bolton, M.D. 1986. The strength and dilatancy of sands. Géotechnique, **36**(1): 65–78.

Bush, D.T., and Swan, D.B.G. 1988. An assessment of the resistance of TENSAR SR2 to physical damage during the construction and testing of a reinforced soil wall. *In* The application of polymeric reinforcement in soil retaining structures. NATO Advanced Study Institutes Series. *Edited by* P.M. Jarrett and A. McGown. Kluwer Academic Publishers, pp. 71–125.

Canadian Geotechnical Society. 2006. Chapter 27: Geosynthetics. *In* Canadian foundation engineering manual, 4th ed. BiTech Publishers, Richmond, B.C.

Hatami, K., and Bathurst, R.J. 2005. Development and verification of a numerical model for the analysis of geosynthetic-reinforced soil segmental walls under working stress conditions. Canadian Geotechnical Journal, **42**(4): 1066–1085.

Hatami, K., and Bathurst, R.J. 2006. A numerical model for reinforced soil segmental walls under surcharge loading. ASCE Journal of Geotechnical and Geoenvironmental Engineering, **132**(6): 673–684.

Holtz, R.D., Christopher, B.R., and Berg, R.R. 1997. Geosynthetic engineering. BiTech Publishers, Richmond, B.C.

Jewell, R.A. 1989. Direct shear tests on sand. Géotechnique, **39**(2): 309–322.

Leshchinsky, D. 2003. Discussion on paper "Peak versus residual shear strength in geosynthetic-reinforced soil design" by J.G. Zornberg. Geosynthetics International, **9**(4): 301–318; Geosynthetics International, **10**(6): 234–237.

McGown, A., Andrawes, K., Yeo, K., and Dubois, D. 1984*a*. The load-strain-time behaviour of Tensar geogrids. *In* Polymer grid reinforcement. Thomas Telford, London, pp. 11–17.

McGown, A., Paine, K., and Dubois, D. 1984*b*. Use of geogrid properties in limit equilibrium analyses. *In* Polymer grid reinforcement. Thomas Telford, London, pp. 31–36.

NCMA. 1997. Design manual for segmental retaining walls, 2nd ed., 2nd printing. National Concrete Masonry Association, Herndon, Va.

Tatsuoka, F. 1993. Roles of facing rigidity in soil reinforcing: Keynote lecture. *In* Proceedings of the International Symposium on

Earth Reinforcement Practice, IS Kyushu 1993, Fukuoka, Japan, 14 November 1993. *Edited by* H. Ochiai, S. Hayashi, and J. Otani.. A.A. Balkema, Rotterdam, The Netherlands, Vol. 2, pp. 831–870.

Walters, D.L., Allen, T.M., and Bathurst, R.J. 2002. Conversion of geosynthetic strain to load using reinforcement stiffness. Geosynthetics International, **9**(5–6): 483–523.

WSDOT. 2005. Determination of long-term strength of geosynthetics, WSDOT test method 925. Washington State Department of Transportation, FOSSC Materials Laboratory, Tumwater, Wash.